

# Structural and optical properties of nanoparticulate $\text{Y}_2\text{O}_3:\text{Eu}_2\text{O}_3$ made by microwave plasma synthesis

A. Kautsch · U. Brossmann · H. Krenn · F. Hofer ·  
D.V. Szabó · R. Würschum

**Abstract** Nanoparticulate  $\text{Y}_2\text{O}_3:\text{Eu}_2\text{O}_3$  with a small, uniform particle size and a well-defined composition was synthesized using a low temperature microwave plasma process. The structural evolution and the luminescence properties were studied in different states of annealing and  $\text{Eu}_2\text{O}_3$  addition using X-ray diffraction, transmission electron microscopy, and UV-photoluminescence spectroscopy. As synthesized, the samples were amorphous and showed only weak luminescence. Subsequent annealing steps from

500°C to 800°C lead to the formation and growth of cubic  $\text{Y}_2\text{O}_3:\text{Eu}_2\text{O}_3$  nanocrystals (5–20 nm) and a concomitant strong increase of the luminescence yield already at small grain sizes in the range of 10 nm. No self-quenching effects were observed up to 11 mol%  $\text{Eu}_2\text{O}_3$ .

## 1 Introduction

Luminescent rare earth oxides are in the focus of both technical application and ongoing research as key materials for use in display technology and lighting [1, 2]. Presently,  $\text{Eu}_2\text{O}_3$ , particularly in form of  $\text{Y}_2\text{O}_3:\text{Eu}_2\text{O}_3$ , constitutes the best red phosphor for fluorescence tubes and plasma display panels to convert UV light from the plasma discharge to red light [1, 3].

$\text{Y}_2\text{O}_3$  and  $\text{Eu}_2\text{O}_3$  preferably form cubic mixed crystals with a high luminescence yield [1–5]. Both, the  $\text{Y}_2\text{O}_3$  host lattice, and  $\text{O}^{2-}$  ions in the vicinity of  $\text{Eu}^{3+}$  ions, absorb UV-light with maxima in the range of 210 nm and 250 nm, respectively. Subsequent energy transfer to the  $\text{Eu}^{3+}$  luminescence centres finally populates the  $5\text{D}_0$  level [1, 3–5]. Red light is emitted upon transition to one of the  $7\text{F}$  levels, with the main emission line at 613 nm ( $5\text{D}_0 \rightarrow \text{F}_2$ ) and weaker lines between 580 and 595 nm [6].

The effect of a very small crystallite size on the luminescence properties, however, remains an open question. On the one hand, some studies report a noticeable blue shift of both the absorption range and the main emission line for particles as large as 40 nm [3, 7]. On the other hand, there are also observations of a red shift of the absorption spectra [4]. Similarly, studies in literature report observations of a reduced [1] as well as an increased luminescence of nanoparticles versus the bulk [8]. In addition, lattice and surface defects were found to significantly impair the luminescence yield

A. Kautsch · U. Brossmann (✉) · R. Würschum  
Institute of Materials Physics, Graz University of Technology,  
8010 Graz, Austria  
e-mail: brossmann@tugraz.at  
Fax: +43-316-8738980

A. Kautsch  
e-mail: andreas.kautsch@tugraz.at

R. Würschum  
e-mail: wuerschum@tugraz.at

### Present address

A. Kautsch  
Institute of Experimental Physics, Graz University of Technology,  
8010 Graz, Austria

H. Krenn  
Institute of Physics, University of Graz, 8010 Graz, Austria  
e-mail: heinz.krenn@uni-graz.at

F. Hofer  
Institute of Electron Microscopy and Fine Structure Research,  
Graz University of Technology, 8010 Graz, Austria  
e-mail: ferdinand.hofer@tugraz.at

D.V. Szabó  
Karlsruhe Institute of Technology, Institute of Applied  
Materials—Materials Process Technology, 76344  
Eggenstein-Leopoldshafen, Germany  
e-mail: dorothee.szabo@kit.edu

of  $Y_2O_3:Eu_2O_3$ , particularly for very small particles [1, 3]. Therefore,  $Y_2O_3:Eu_2O_3$  nanoparticles with a low degree of internal strains and agglomeration are expected to show improved luminescence.

The present work aims at synthesizing and studying the structural and luminescence properties of such  $Y_2O_3:Eu_2O_3$  nanoparticles with a small initial particle size. For this goal, microwave plasma (MWP) synthesis provides an ideal fabrication route [9]. The low reaction temperature of about  $400^\circ C$  and the electric charging in the nonequilibrium plasma leads to the formation of nanoparticles with both a small mean size of  $d \sim 4\text{--}5$  nm and a narrow size distribution.

## 2 Experimental

The nanoparticulate  $Y_2O_3:Eu_2O_3$  was produced by co-evaporation of the chemically homologous tetramethylheptanedionate  $Y(TMHD)_3$  and  $Eu(TMHD)_3$  precursors in an Ar stream at about  $180^\circ C$ . The precursor vapor was mixed with a reaction gas of 20% oxygen in argon and then decomposed in the microwave induced plasma (2.45 GHz, 500 W) under similar conditions as described for the synthesis of YSZ [9]. Electric charging induced by the plasma together with low reaction temperatures prevents the formation of hard agglomerates. The nanoparticles were collected on a cold finger. This powder was subsequently scraped off with a razor blade and placed in an  $Al_2O_3$  boat for annealing treatments at temperatures between  $350^\circ C$  and  $800^\circ C$  in air.

X-ray diffraction studies of the structural evolution of nanoscaled (n)- $Y_2O_3:Eu_2O_3$  powders were made using a Bruker D8 Advance instrument with a Cu tube. For transmission electron microscopy (TEM) studies using a Philips CM20 microscope, the n- $Y_2O_3:Eu_2O_3$  powder was dispersed in 2-Propanol and deposited on a Cu grid.

Photoluminescence (PL) studies on n- $Y_2O_3:Eu_2O_3$  and the pure constituents were carried out on both powder samples on glass and dispersions in ethanol (0.5 g/l). The luminescence spectra were measured with a Perkin-Elmer LS55 spectrometer using a high-energy pulsed Xe lamp as light source. A filter with a cut-off wavelength of 570 nm prevented spurious light from entering the analyzer.

Two types of PL spectra were recorded for samples in all conditions of annealing and compositions: emission spectra of luminescence induced by excitation at fixed wavelengths of 211 and 234 nm and so-called excitation spectra, which show the intensity of the main PL emission line at 613 nm as a function of the excitation wavelength. A wavelength scan rate of 100 nm/min and bandwidths of 5 nm and 2.5 to 5 nm for excitation source and analyzer, respectively, were typically used for these measurements.

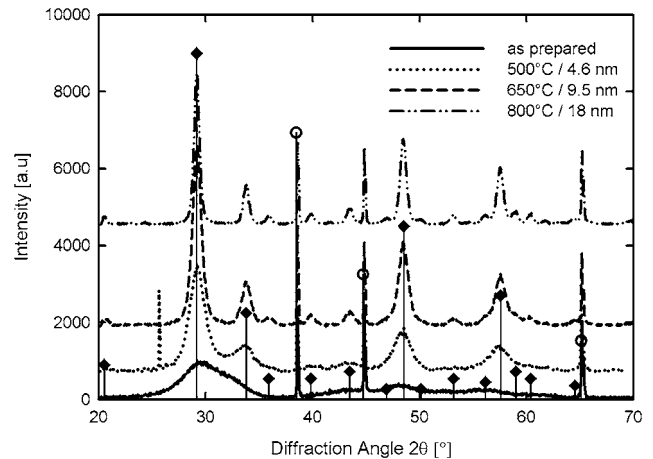


**Fig. 1** X-ray diffraction spectra of  $Y_2O_3:Eu_2O_3$  in different stages of annealing. The symbols  $\blacklozenge$  and  $\circ$  denote literature data for  $Y_2O_3:Eu_2O_3$  (5 mol%) and Al (specimen holder) from the PDF-2 database, respectively [10]. No noticeable change is observed for samples with  $Eu_2O_3$  addition of 5.6 and 11 mol%

## 3 Results and discussion

Under as-synthesized condition, both  $Eu_2O_3$  doped (Fig. 1) and undoped  $Y_2O_3$  nanoparticles show broad X-ray diffraction lines. In complementary TEM studies a small particle size and loose agglomerates of particles with nearly missing crystalline features were observed (Fig. 2a). Hence, an amorphous state with an average particle size of about 4.5 nm is deduced. Annealing at  $350^\circ C$  did not induce a significant change in the structural properties. Annealing at  $500^\circ C$  for 8 h lead to the formation of cubic nanocrystals of an  $Y_2O_3:Eu_2O_3$  solid solution (Fig. 1) or  $Y_2O_3$ , as shown by XRD. These data are consistent with literature data for bulk  $Eu_{0.1}Y_{1.9}O_3$  (JCPDS #25-1011) and  $Y_2O_3$  (JCPDS #88-1040) in the PDF-2 database [10], respectively. No evidence for the formation of pure cubic  $Eu_2O_3$  or monoclinic phases was found.

From the XRD data, a small average crystallite size of  $4.6 \pm 0.5$  nm is determined based on the Scherrer formula [11], whereas a detailed analysis using the approach of Williamson–Hall [11] yields a value of  $6.5 \pm 0.5$  nm and indicates a noticeable amount of microstrains. Additional annealing at  $650^\circ C$  or  $800^\circ C$  (4 h) lead to crystallite growth reaching values of  $9.5 \pm 0.5$  nm and  $18 \pm 1$  nm, respectively. For samples annealed at  $800^\circ C$ , the crystallite size and the crystalline state was confirmed by TEM studies (Fig. 2b).

Experimental data of the luminescence properties of  $Y_2O_3:Eu_2O_3$  in dispersions are shown in Figs. 3, 4, and 5. In condition as synthesized and after annealing at  $350^\circ C$ , the n- $Y_2O_3:Eu_2O_3$  specimens showed only weak luminescence due the reduced energy transfer in the amorphous structure [12]. After annealing at  $500^\circ C$ , the typical luminescence spectrum of  $Eu^{3+}$  was observed (Figs. 3, 4).

**Fig. 2** TEM micrographs of (a)  $\text{Y}_2\text{O}_3:\text{Eu}_2\text{O}_3$  as synthesized and (b) after the annealing step at  $800^\circ\text{C}$  (4 h, air)

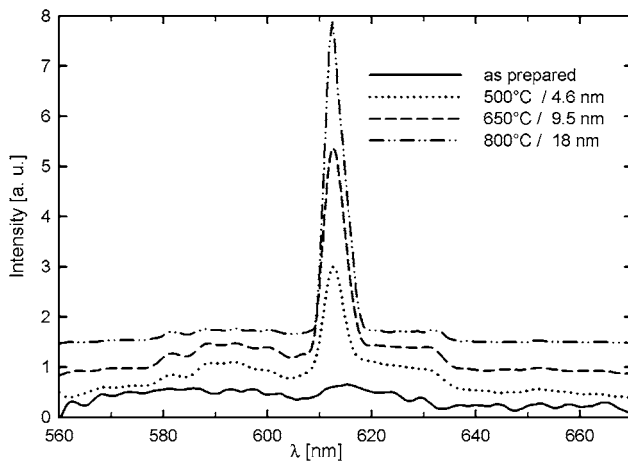
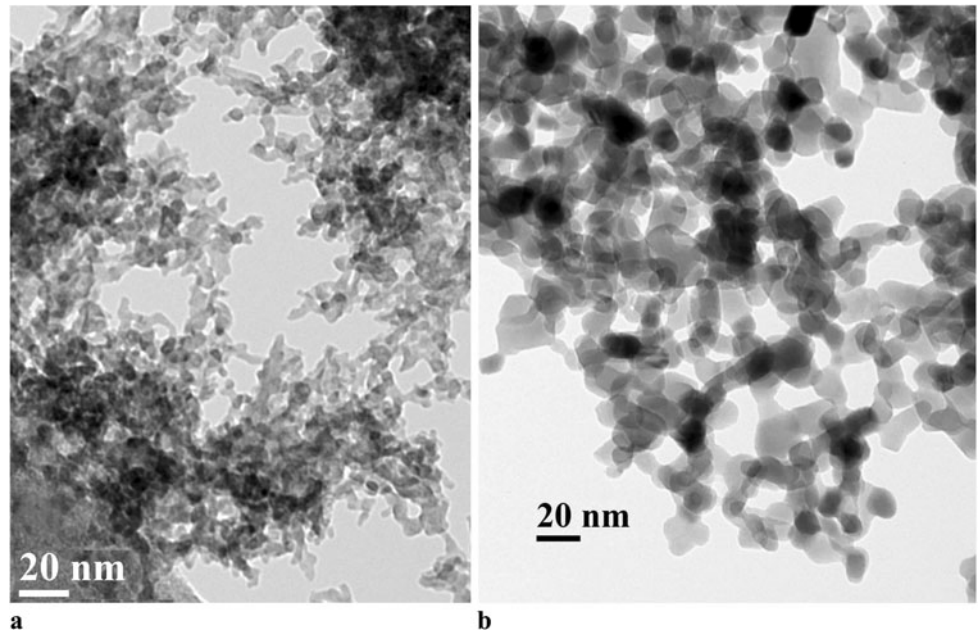


**Fig. 3** Luminescence spectra of  $n\text{-Y}_2\text{O}_3:\text{Eu}_2\text{O}_3$  (11 mol%) in dispersion upon excitation with wavelength  $\lambda_{\text{ex}} = 234$  nm in different states of annealing. The plots are mutually shifted in vertical direction. The crystallite size is deduced from XRD line broadening (Scherrer)

Higher annealing temperatures of  $650^\circ\text{C}$  and  $800^\circ\text{C}$  lead to a strong increase of the luminescence yield, but to no qualitative change in the excitation and emission spectra such as shifts of the peaks with the grain size.

Taking into account the structural data (s. Figs. 1, 2) it may be concluded in agreement with literature data that a crystalline state is essential for the photoluminescence and UV conversion processes in  $\text{Y}_2\text{O}_3:\text{Eu}_2\text{O}_3$  [3–7]. In fact, the PL yield is reduced for ultra small grain sizes (Figs. 3–5). However, we observed a significant PL yield already at crystallite sizes in the range of 5–10 nm (Fig. 3), smaller than previously reported [3].

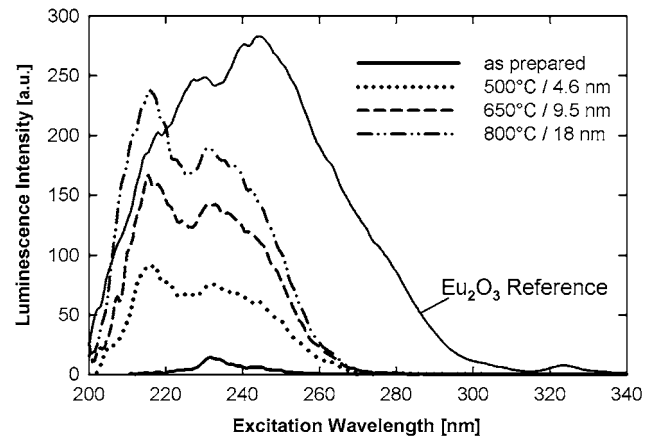


**Fig. 4** Excitation spectra for the luminescence at  $\lambda_{\text{em}} = 613$  nm ( $5\text{D}_0 \rightarrow 7\text{F}_2$ ) measured on dispersed  $\text{Y}_2\text{O}_3:\text{Eu}_2\text{O}_3$  particles. Bulk  $\text{Eu}_2\text{O}_3$  is shown as a reference

A detailed look at the excitation spectra of  $n\text{-Y}_2\text{O}_3:\text{Eu}_2\text{O}_3$  specimen (Fig. 4) shows two maxima for wavelengths of about 211 nm and 234 nm in the far UV range, which can be attributed to the host-lattice and charge transfer mechanisms, respectively [3–5]. The PL yield for both excitation wavelengths increases with the grain size (Fig. 4, Fig. 5) as well as with the  $\text{Eu}_2\text{O}_3$  content (Fig. 5). Hardly any PL is observed for the as prepared  $n\text{-Y}_2\text{O}_3:\text{Eu}_2\text{O}_3$  specimen at  $\lambda_{\text{ex}} < 220$  nm (Fig. 4). With higher annealing temperatures and crystallite size the excitation at  $\lambda_{\text{ex}} = 211$  nm, corresponding to the host lattice transfer, becomes more dominant in comparison to  $\lambda_{\text{ex}} = 234$  nm, which may reflect a more efficient host-lattice energy transfer in larger grains [1, 3–5]. It is also interesting to note, that the relative intensity of the main emission line, which is attributed to  $\text{Eu}^{3+}$

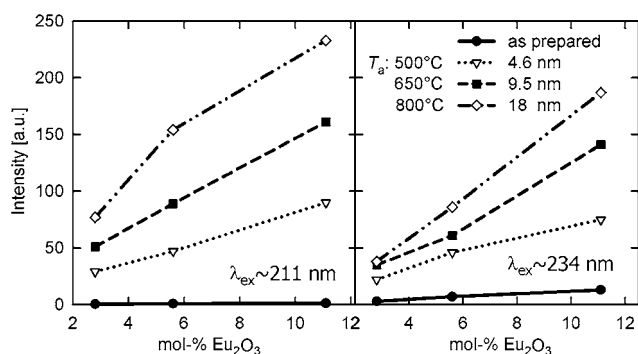


**Fig. 5** Variation of photoluminescence yield in  $Y_2O_3:Eu_2O_3$  with annealing treatment and  $Eu_2O_3$  content for regions of host lattice ( $\lambda_{ex} = 211$  nm) and charge transfer excitation ( $\lambda_{ex} = 234$  nm)

emission centres in an undistorted cubic lattice environment [13], increases for higher annealing temperatures (Fig. 3).

These improved luminescence properties may be attributed to a reduced density of lattice and surface defects as a result of the synthesis method used [12].

No evidence for self-quenching was observed for any state of annealing or  $Eu_2O_3$  content up to the highest doping level of 11 mol% studied. For bulk material, such a quenching effect was reported for  $Eu_2O_3$  additions to  $Y_2O_3$  as low as 6% [14]. Assuming an isotropic distribution of  $Eu^{3+}$  in the nanocrystals, the reduced self-absorption may be attributed to the large fraction of luminescence centers located directly at the nanoparticles' surface, which is expected to reduce this doping-dependent critical effect.

Based on these results, it can be concluded that microwave plasma synthesis combined with appropriate annealing is a powerful technique for the fabrication of oxide rare earth nanoparticles, which combine a well-defined small size and composition with good luminescence properties. Nevertheless, the present study confirms that the luminescence yield of  $Y_2O_3:Eu_2O_3$  is reduced for very small

grain sizes. Slightly larger grains ( $d \geq 9.5$  nm) with a high degree of crystallinity show a promising luminescence yield tendency.

**Acknowledgements** The authors thank A. Meingast, Graz University of Technology, for TEM micrographs and S. Draxler, University of Graz for technical support.

## References

1. R. Schmechel, M. Kennedy, H. von Seggern, H. Winkler, M. Kolbe, R.A. Fischer, Li Xiaomao, A. Benker, M. Winterer, H. Hahn, *J. Appl. Phys.* **89**, 1679 (2001)
2. P.K. Sharma, M.H. Jilavi, R. Nass, H. Schmidt, *J. Lumin.* **82**, 187 (1999)
3. A. Konrad, T. Fries, A. Gahn, F. Kummer, U. Herr, R. Tidecks, K. Samwer, *J. Appl. Phys.* **86**, 3129 (1999)
4. Q. Meng, C. Qingyu, B. Chen, X. Zhao, X. Wang, W. Xu, *J. Nanosci. Nanotechnol.* **8**, 1443 (2008)
5. A. Konrad, U. Herr, R. Tidecks, F. Kummer, K. Samwer, *J. Appl. Phys.* **90**, 3516 (2001)
6. G. Wakefield, E. Holland, P.J. Dobson, J.L. Hutchison, *Adv. Mater.* **13**, 1557 (2001)
7. Q. Li, L. Gao, D. Yan: *Nanostruct. Mater.* **8**, 825 (1997)
8. E.T. Goldburt, B. Kulkarni, R.N. Bhargava, J. Taylor, M. Libera, *J. Lumin.* **72–74**, 190 (1997)
9. U. Brossmann, M. Sagmeister, P. Pölt, G. Kothleitner, I. Letofsky-Papst, D.V. Szabó, R. Würschum, *Phys. Status Solidi RRL* **1**, 107 (2007)
10. PDF-2, *The Powder Diffraction File Rel. 2001* (The International Center for Diffraction Data, Newtown Square, 2001)
11. H.P. Klug, L.E. Alexander, *X-ray Diffraction Procedures for Polycrystalline and Amorphous Materials*, 2nd edn. (Wiley, New York, 1974)
12. R. Schmechel, H. Winkler, Li Xiaomao, M. Kennedy, M. Kolbe, A. Benker, M. Winterer, R.A. Fischer, H. Hahn, H. von Seggern, *Scr. Mater.* **44**, 1213 (2001)
13. S.C. Cho, H.S. Uhm, C.U. Bang, D.K. Lee, C. Soo, *Thin Solid Films* **517**, 4052 (2009)
14. X. Ye, W. Zhuang, Y. Hu, T. He, X. Huang, C. Liao, S. Zhong, Z. Xu, H. Nie, G. Deng, *J. Appl. Phys.* **105**, 064302 (2009)